ELSEVIER

Journal of Photochemistry and Photobiology A: Chemistry 148 (2002) 137–143

Journal of Photochemistry and Photobiology A:Chemistry

www.elsevier.com/locate/jphotochem

The effect of operational parameters on the photocatalytic degradation of humic acid

Fiona L. Palmer [a,*], Brian R. Eggins [b], Heather M. Coleman [c]

[a] *School of Information and Software Engineering, University of Ulster, Cromore Road, Coleraine, Co. Londonderry BT52 1SA, Ireland*
[b] *School of Applied Medical and Sports Studies, University of Ulster at Jordanstown, Shore Road, Newtownabbey, Co. Antrim BT37 0QB, Ireland*
[c] *Queen's University at Belfast, Co. Antrim, Ireland*

Received 24 July 2001; received in revised form 19 November 2001; accepted 19 November 2001

Abstract

This work investigated the potential of semiconductor photocatalysis for the treatment of drinking water. More specifically it determined the effect of the following operational parameters on the adsorption, rate of initial degradation, and mineralisation of Aldrich humic acid solutions: concentration, temperature, oxygen, light intensity, and pH.

The kinetics of humic acid degradation were found to be complex due to the heterogeneity and high molecular weight of these compounds. Models which are often applied to semiconductor photocatalysis did not fit; the high adsorption of humic acid on the titanium dioxide surface needed to be taken into account. © 2002 Published by Elsevier Science B.V.

Keywords: Humic acid; Semiconductor photocatalysis; Operational parameters

1. Introduction

Humic substances may be classed as group of heterogeneous polymeric organic acids. They are yellow to black in colour and have high molecular weights (100 to several thousand daltons). In 1993, Schulten et al. [1] proposed a tentative structure for these humic substances. They reported a flexible network of aromatic chains bonded by long-chain alkyl structures.

Humic substances in drinking water were initially removed because they impart a colour to the water that is not aesthetically pleasing to domestic consumers. The colour also renders it unsuitable for the paper, beverage and textile industries. However it is also well established that humic substances upon chlorination (used for disinfection purposes) form mutagenic halogenated compounds. Numerous reports have demonstrated the formation of trihalomethanes, haloacetonitriles, haloacetic acids, and MX (3-chloro-4-(dichloromethyl)-5-hydroxy-2(H)-furanone) a highly reactive and unstable furanone derivative. It is therefore imperative that the concentration of humic substances should be drastically reduced in raw drinking waters before chlorination begins.

We have been studying the oxidative technology called semiconductor photocatalysis. This uses a solid semiconductor and near ultra-violet light to degrade organic substrates. Normally titanium dioxide is used as the semiconductor. In our previous work [2] we demonstrated that semiconductor photocatalysis could degrade humic substances in drinking water via a series of lower molecular weight intermediates to carbon dioxide and water. Other researchers [3] have since published work in this area including the researcher Bekbolet [4–7].

If we are to evaluate the potential of semiconductor photocatalysis as an alternative drinking water treatment process then it is essential that the effects of various operational parameters are investigated. The overall aims and objectives of this study were therefore to: '*investigate the effect of the following operational parameters on the adsorption, initial degradation and mineralisation rate of humic acid, in a suspension photocatalytic reactor: concentration, temperature, oxygen, light intensity, and pH*'.

2. Experimental

2.1. Humic acid and semiconductor source

Commercially sourced humic acid from Aldrich was used, allowing the composition to be controlled (sodium salt, lot

* Corresponding author. Tel.: +44-28-7032-3012.
E-mail address: fiona@causeway.infc.ulst.ac.uk (F.L. Palmer).

1010-6030/02/$ – see front matter © 2002 Published by Elsevier Science B.V.
PII: S1010-6030(02)00083-7

number 61052-124). The only pre-treatment was filtration through 0.22 μm millipore filters. The semiconductor (Degussa P-25) was used in the form of a 0.1% suspension.

2.2. Irradiation experiments

The reactor consisted of a 100 cm^3 round bottomed Pyrex flask. Influent gases (oxygen free nitrogen or oxygen from BOC, or air from an aerator) were bubbled through the reactor after passing through saturated barium hydroxide (AnalaR grade, BDH), and dilute sulphuric acid (BDH, ConVol), ensuring that the inlet gases were carbon dioxide free. The effluent gases were bubbled through a conductivity cell to allow the determination of the extent of mineralisation. Irradiation was performed with a 250 W medium pressure mercury arc lamp (mainline of emission 365 nm from Thorn-EMI) with a 250 W power supply (Applied Photophysics) linked to a voltage stabiliser (Claude Lyons TS1). Oxygen experiments were conducted using a 400 W metal halide lamp (HPA 400F), mainline of emission 365 nm.

Thirty minutes were allowed for equilibration in the dark so that adsorption could occur before irradiation. During equilibration the gas to be used was bubbled through and the lamp allowed to warm. During irradiation samples were withdrawn and filtered through 0.22 μm pore size filters to remove the titanium dioxide. Not more than 10% of the total volume was withdrawn throughout any one experiment. Experiments without titanium dioxide present were also performed for each set of experiments. No significant degradation was observed. The potassium ferrioxalate liquid chemical actinometer, developed by Hatchard and Parker [9,10], was used to determine light intensities within the reactor.

2.3. Analysis of humic acid concentrations

Analysis was performed only by high performance size exclusion chromatography (HPSEC), due to the low sample volume required. The equipment included: pump (Spectra Physics Spectra System P2000 or a Shimadzu LC-6A); Column Chiller (Jones Chromatography M7955); Column (TSK gel G3000 SW) (300 mm × 7.5 mm); Detector (Spectra Focus optical scanning UV/visible variable wavelength detector); Data Acquisition Software (Spectra Physics Spectra Focus). The conditions are detailed as follows: mobile phase (0.1 M, pH 6.8 sodium acetate); flow rate (1 $cm^3\ min^{-1}$); pressure (300 psi); sample loop (1 cm^3), average run time (30 min). These conditions are similar to those used by Backlund et al. [8] in their analysis of the degradation of humic acid by ultra-violet light.

Correlations between peak area, measured at 254 nm, and dissolved organic carbon (DOC) content were made from a standard curve constructed by measuring the DOC of a range of humic acid solutions. The measurement of DOC was performed with a Shimadzu Total Organic Carbon Analyser (5050A).

2.4. Determination of the extent of mineralisation

Mineralisation was determined by measuring the carbon dioxide released from the reactor. The effluent gas was passed through a conductivity cell containing a 0.005 M barium hydroxide solution (AnalaR grade, BDH) and measuring the conductivity drop.

3. Results and discussion

3.1. Attainment of equilibrium

The researcher Chen et al. [11] was interested in the effect of mass transfer or adsorption onto the surface of the semiconductor. He developed equations to describe the effect of mass transfer on the rate of photocatalysis. He suggested that experiments reported to behave according to a Langmuir–Hinselwood mechanism could be partially or totally controlled by mass transfer phenomena.

3.1.1. Rate of equilibration

In order to determine the rate of attainment of equilibrium in the dark the concentration of humic acid in the bulk solution was determined at various times during equilibration in the dark. The results are shown in Fig. 1. Equilibration was achieved in approximately 20 min. A plot of $\ln([S]_{ads}^{t=t_{eq}} - [S]_{ads}^{t=t_{ads}})$ against time, t, before equilibrium, where $[S]_{ads}^{t=t_{eq}}$ is the amount of substrate adsorbed at equilibrium and $[S]_{ads}^{t=t_{ads}}$ is the amount of substrate adsorbed after the start of the adsorption period, was plotted (not shown). The kinetic constant, k_{MT}, for adsorption was estimated to be 0.11 min^{-1} from the slope (according to Chen et al. [11]). This is slightly higher than that reported by Chen for trichloroethylene: 0.0813–0.0871 min^{-1} for concentrations between 0.05 and 1.50 $mmol^{-1}$.

3.1.2. Fraction of humic acid adsorbed to the surface

At equilibrium 58.1% of the initial concentration was adsorbed onto the titanium dioxide. This is a high proportion compared to other substrates such as phenol for which less

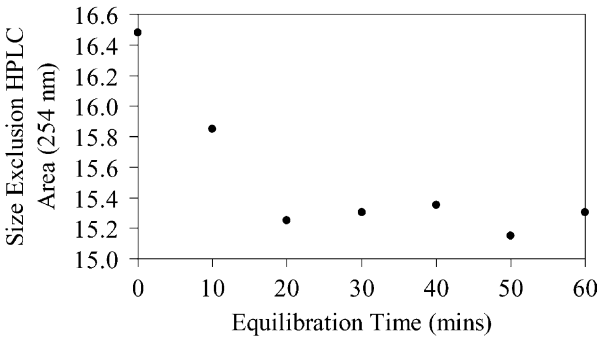

Fig. 1. Adsorption of humic acid over time in the dark.

than 5% adsorption has commonly been reported. Humic acid being of a relatively large size and having more functional groups than phenol per molecule may be expected to show a higher adsorption.

3.2. Effect of concentration

The main effect of increasing concentration is to increase the amount of substrate, *S*, that is adsorbed onto the semiconductor surface. Most researchers have applied the Langmuir model to semiconductor adsorption in which a monolayer is assumed. Once this layer has been formed a saturation point is reached above which no further adsorption can occur. If we assume photocatalysis occurs at the surface, then the concentration of substrate adsorbed to the surface directly affects the overall rate of adsorption. Assuming that the concentration of oxidant is unaffected by the substrate the reaction can be deemed to be pseudo first-order. A model based on these assumptions, the Langmuir–Hinshelwood model, has been used by many researchers to describe semiconductor photocatalysis kinetics [12]:

$$\text{initial rate} = \frac{k_s K_s [S]_{eq}}{1 + K_s [S]_{eq}} n_{max} W$$

where k_s is the measure of the intrinsic reactivity of oxidant with substrate; $[S]_{eq}$ the concentration of substrate at equilibrium in the bulk solution; K_s the Langmuir adsorption constant of the substrate *S* on the semiconductor surface; n_{max} the total number of adsorption sites accessible to the substrate; *W* the catalyst loading.

3.2.1. Adsorption

Initial experiments to determine the effect of concentration on the adsorption of humic acid using the standard technique of varying the humic acid concentration proved difficult. The problems concerned the aggregation of the humic acid at high concentrations, and detection limits at lower concentrations (especially after adsorption). Thus a novel approach was tested. Instead of varying the humic acid concentrations the titanium dioxide concentrations were varied.

A graph of the amount of humic acid adsorbed against the equilibrium concentration is shown in Fig. 2. A plot of $[S]_{eq}/([S]_{ads}/W)$ (where $[S]_{ads}$ the concentration of substrate adsorbed onto the semiconductor surface) against $[S]_{eq}$ was drawn. From the plot K_s and n_{max} were calculated, from the gradient and the slope respectively, according to the method described by Cunningham et al. [12]. The results are shown in Table 1 where a comparison has been made with salicyclic acid (often used as a model for humic acid).

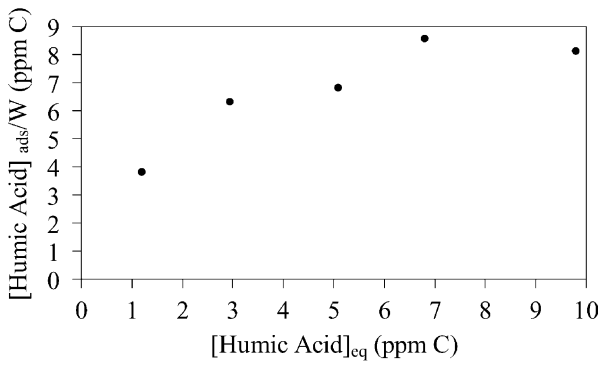

Fig. 2. Concentration of humic acid adsorbed per mass of titanium dioxide against the equilibrium concentration of humic acid.

From Table 1 we see that K_s, a measure of the affinity of a humic acid molecule for titanium dioxide was determined to be: $2.306\,dm^3\,mol^{-1} \times 10^{-3}$. This value for K_s was approximately 200 times higher than that previously reported for salicyclic acid. This might be expected; the humic acid molecule is a high molecular weight compound, with a larger number of functional groups per molecule (and thus binding opportunities) compared to salicyclic acid. The affinity in terms of amount of carbon is at least six times as high as salicyclic acid. This is probably due to the fact that in the case of humic acid, where potentially at least an entire molecule could be attached by one functional group, a larger amount of carbon can be attached per binding site.

The value for n_{max}, the saturation point, was determined to be 0.0026 mmol/g TiO_2. This was approximately 30 times lower than that previously reported for salicyclic acid. As the humic acid is large it would be expected that the number of molecules that could bind before saturation is reached would be lower. The molecule may for instance bind to several sites at once or block other binding sites. The value for n_{max}, in terms of amount of carbon, is actually higher for humic acid. This again might be expected due to the 3D shape of humic acid and the possibility that only part of the structure is attached to the surface with the other section lying such that other molecules can bind at adjacent sites on the titanium dioxide.

Table 1
Table of values of K_s and n_{max} for Aldrich humic acid derived from linearised Langmuir–Hinshelwood plots using data acquired from $HPSEC_{254}$ measurements and by varying the titanium dioxide concentration

	n_{max} (mmol/g TiO_2)	K_s ($dm^3\,mol^{-1}$) $\times 10^{-3}$	n_{max} (mg C/g TiO_2)	K_s (dm^3 per mg carbon) $\times 10^{-3}$
Aldrich humic acid	0.0026[a]	2.306[a]	9.68	0.624
Salicyclic acid	0.0704	10.5	5.91	0.125

[a] In the calculation an estimation of the number of moles of humic acid was determined by assuming that each humic acid molecule contained 308 carbons; this is the number of carbons in the tentative structure for humic acid suggested by Schulten et al. [1].

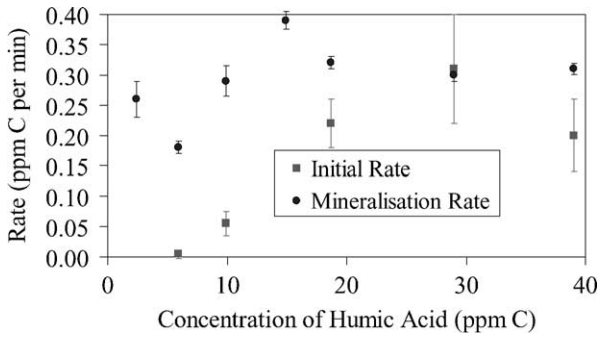

Fig. 3. Effect of concentration on the initial rate of degradation and mineralisation of humic acid.

3.2.2. Initial degradation

The effect of concentration on the initial rate of humic acid degradation did not appear to follow the standard Langmuir–Hinshelwood kinetics commonly applied in semiconductor photocatalysis experiments (Fig. 3). The rate of degradation does increase with increasing concentration until the concentration of 30 ppm carbon, but after this concentration the rate actually decreased. Ignoring the point after 30 ppm carbon, we observe that the plot does not show the typical convex curve of a reaction controlled by Langmuir–Hinshelwood kinetics but is actually slightly concave in nature. We believe these unusual results are due to several factors. The complex shape can be attributed to the relatively high adsorption of humic acid (over 50%), and other various effects at high concentrations.

To explain the shape of this rate versus concentration plot consider again the parameters involved in a Langmuir–Hinshelwood plot. In the Langmuir–Hinshelwood model the rate of change in the *total* concentration of substrate is directly proportional to the amount of substrate adsorbed at the surface. However when we measure rates we typically measure the rate of change in the *bulk* solution. In the case of substrates that demonstrate very low adsorption onto the surface (such as phenol), the difference between the rate of reduction in the bulk and in total would be relatively insignificant. In the case of humic acid, which may show adsorption percentages up to 100 times greater than some substrates, this effect is no longer negligible especially in the lower concentration range. At lower concentrations the amount adsorbed at the surface decreases with decreasing equilibrium concentrations, acting to lower rates observed in the bulk solution. Models have been developed taking into account this adsorptive effect and will be published in a later paper [13].

The reduction in rate above 30 ppm C is a more complex issue. A light screening effect was determined but dismissed as insignificant. The recombination of radicals may playing a role: at these high concentrations the chances of intermediate species reacting to form molecules of a higher molecular weight is more likely. In previous experiments it was suggested that indeed intermediates from humic acid photocatalysis experiments may combine with one another forming larger structures [13]. It was also noted that at the highest concentrations the aggregation of humic acid and titanium dioxide appeared to occur very rapidly on irradiation. This may be expected as the humic acid solution was close to its solubility range and the titanium dioxide was effectively acting as a coagulating agent; this was deemed to be the most important factor.

Bekbolet and Ozkoswman [4] did not report any such problems in similar experiments with a humic acid sourced from roth. They determined rates by measuring the reduction in TOC, COD, $UV_{254\,nm}$, and $colour_{400\,nm}$ over time and obtained excellent fits to the Langmuir–Hinshelwood model.

3.2.3. Mineralisation

The steady state rate of mineralisation did not change significantly with increasing concentration suggesting zero order kinetics for carbon dioxide production (Fig. 3). The rates are similar to those obtained for phenol in the same reactor by a previous researcher (approximately $0.2\,ppm\,C\,min^{-1}$ above an apparent saturation level of 14.4 ppm C) [14]. These zero order kinetics could be attributed to a rate determining oxidation of an intermediate en-route to carbon dioxide.

Mineralisation is a complex process and more sophisticated models taking into account intermediates, have been developed to describe the results, such as those developed by Matthews and Mc Evoy [15], and Serpone and co-workers [16,17]. Mills et al. [18] also built models describing the mineralisation of salicyclic acid and 4-chlorophenol [19] based on a knowledge of the major intermediates of degradation and assuming several routes of mineralisation.

3.3. Effect of temperature

3.3.1. Adsorption

There was little change in adsorption and hence the adsorption coefficient over the temperature range studies (10–68 °C) thus it might be expected that adsorption will not affect initial degradation rates for humic acid; the effect on intermediate adsorption en-route to carbon dioxide remains unknown.

3.3.2. Initial degradation rates and mineralisation

The rate of initial degradation and mineralisation fluctuated with increasing temperature (results not shown). There was approximately a two fold increase in rate for both initial degradation and mineralisation from the minimum to the maximum rate. No significant trends over temperature were demonstrated. Many researchers have applied the Arrhenius theory to describe the effect temperature has on the rate constant of the reaction between the substrate and the oxidising species, k_s. Our data did not fit the Arrhenius equation well, so no results are shown.

These results are not surprising when we consider the number of different and conflicting effects that temperature

can have on semiconductor photocatalysis. Temperature for instance can increase the interfacial charge transfer rate [20] by changing the number of charge carriers and the rate constant. It may also serve to increase the mass transfer rate (although this will only affect the overall rate if it is rate limiting) and the rate of indirect oxidation in homogenous solution. Temperature will act to lower the concentration of oxygen in solution which may limit rates [21]. It also affects the adsorption and desorption of intermediates [22] (more tending to be adsorbed at lower temperatures), which compete with the initial substrate.

3.4. Light intensity

3.4.1. Adsorption

The amount of adsorption at different light intensities cannot be determined directly.

3.4.2. Initial degradation and mineralisation

As light intensity increases, the rate of degradation also increases due to the increasing number of oxidising species (Fig. 4). There appear to be two regions one above and one below 1.22×10^{-5} einsteins s^{-1}; in each region an increase in light intensity results in differing degrees of rate increase:

- At lower light intensities the rate of initial degradation increases in proportion to light intensity suggesting that few oxidising species are lost through recombination processes.
- At higher light intensities the rate of initial degradation increases in proportion to light intensity to a power of 0.12 and the rate of mineralisation rises in proportion to light intensity to the power of 0.58. This results in lower and lower quantum yields as light intensity increases, as recombination effects become more significant and mass transfer becomes rate limiting.

Quantum yields (0.003–0.039 mol of carbon per photon) are similar to those obtained by earlier researchers (0.0035 reported by Mills et al. [18] for salicyclic acid) and are relatively low. The transition point observed at 1.22×10^{-5} einsteins s^{-1} is approximately 20 times lower than that observed by Okamoto et al. [23] during the degradation of phenol (2×10^{-4} einstein s^{-1}).

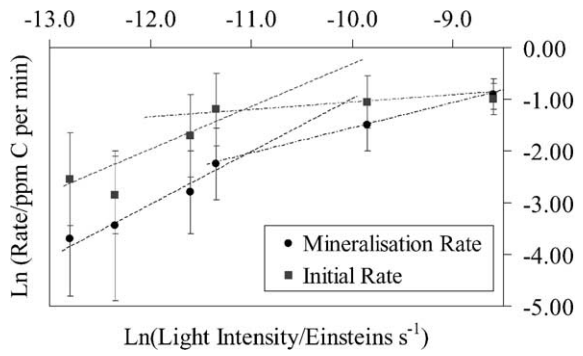

Fig. 4. The effect of light intensity on the initial rate of degradation and mineralisation of humic acid.

One of the other interesting factors is the ratio of the rate of mineralisation to initial degradation rate. Above the transition light intensity the ratio of the steady state mineralisation rate to the initial degradation rate increases. Augugliaro et al. [24] who investigated the effect of light intensity on the photocatalysis of 4-chlorophenol found an enhanced rate of mineralisation relative to initial substrate decay at lower light intensities. They suggested that the slower rate of hole formation may allow the intermediates in solution to come to an adsorption equilibrium. In our case the effect is opposite and may be due to intermediates (with a low affinity for titanium dioxide in comparison to humic acid) desorbing into the bulk before they can be oxidised on the surface. At higher light intensities they may not desorb fast enough to prevent their oxidation at the surface.

3.5. Oxygen

Adsorbed oxygen due to its availability in water often serves as the electron acceptor in semiconductor photocatalysis. Rate equations have been derived assuming a Langmuir adsorption of oxygen onto the titanium dioxide surface [25]. Hoffmann and co-workers [26] reported that the rate of oxidation was independent of oxygen concentrations below air saturation values, and Upadhya and Ollis [27] suggested that the mass transfer of oxygen to the surface could be rate limiting.

The role of oxygen may not merely be one of an electron acceptor. Oxygen for instance may be involved in the formation of other oxidative species (superoxide, hydrogen peroxide, hydroxyl radicals), in the prevention of reduction reactions, in the stabilisation of radical intermediates, mineralisation, and direct photocatalytic reactions.

3.5.1. Adsorption

Values for K_s and n_{max} were determined for Aldrich humic acid under oxygenated, aerated and nitrogen atmospheres (Table 2). There is a smaller value for K_s under nitrogen. But overall oxygen did not affect the adsorption isotherms significantly. This may indicate that, as previously reported by other researchers, oxygen does not compete with the substrate but is adsorbed at different sites.

Table 2
Table of values of K_s and n_{max} for Aldrich humic acid derived from linearised Langmuir–Hinshelwood plots using data acquired from $HPSEC_{254}$ measurements and by varying the titanium dioxide concentration

Atmosphere	n_{max} (mg C/g TiO_2)	K_s (dm^3 per mg carbon) $\times 10^{-3}$
Oxygen	9.86	0.624
Nitrogen	10.7	0.373
Air	8.07	0.623

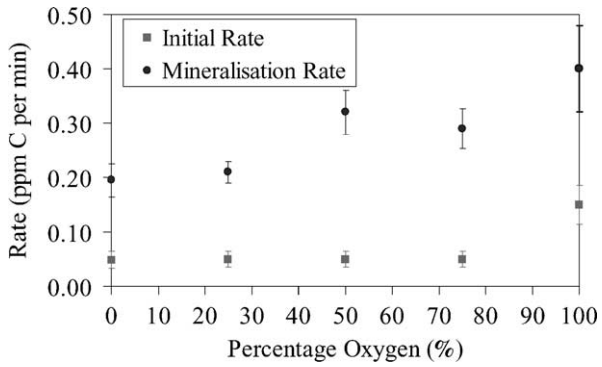

Fig. 5. The effect of oxygen on the initial rate of degradation and mineralisation of humic acid.

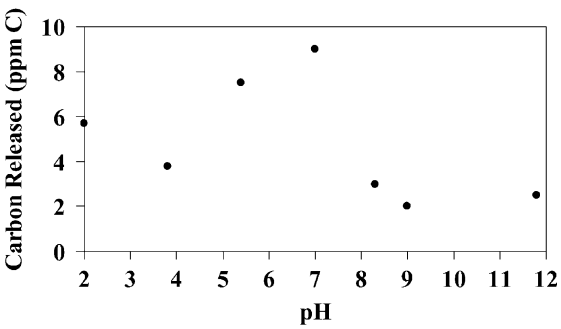

Fig. 6. The effect of pH on the mineralisation of humic acid.

3.5.2. Initial degradation and mineralisation

Fig. 5 shows the initial degradation and mineralisation rates under different influent oxygen compositions. It is immediately apparent that the data does not follow the typical convex relationship expected of a Langmuir–Hinshelwood model (relating the amount of oxygen adsorbed to the rate) although in general the rate did increase with increasing oxygen concentrations. The initial rate of degradation below oxygen compositions of 75% match the results found by Hoffmann and co-workers [26], where rate is independent of oxygen below air saturation values.

When the experiment was performed under nitrogen initial degradation and mineralisation was still observed. In previous research we showed that phenol did not degrade or mineralise under nitrogen [28]. Degradation did occur if alternative electron acceptors were present, however no carbon dioxide was released suggesting oxygen was required for mineralisation. In these studies the initial degradation rates indicate that something is acting as an alternative electron acceptor. There are a few possibilities including metal ions which often bind to humic acids and can be present as impurities, and humic acid itself which contains quinone type structures.

The mineralisation rates that we observed under nitrogen may be due to the oxidation of aliphatic chains. In our previous work we deemed that oxygen was necessary for mineralisation of phenol. This was not the case for the following aliphatic acids: oxalic, muconic, and maleic and fumaric,

Table 3
Summary of results for the effect of operational parameters on the adsorption, degradation, and mineralisation of Aldrich humic acid by semiconductor photocatalysis (0.1% suspension of titanium dioxide; 250 W mercury lamp except for oxygen experiments which used a 400 W metal halide lamp)

Experiment	Range of values	Results
Rate of equilibration	15.5 ppm C solution, room temperature	Mass transfer rate: 0.11 min^{-1}
Concentration and adsorption	4.72–39.3 ppm C solutions	K_s: 0.624 dm^3 per mg carbon × 10^{-3} n_{max}: 9.68 mg C/g TiO_2
Concentration and initial degradation	2.72–39.3 ppm C solutions	Did not follow the standard Langmuir–Hinshelwood model
Concentration and mineralisation	2.72–39.3 ppm C solutions	Apparent zero order kinetics
Temperature and adsorption	15–78 °C, 5.5 ppm C solutions	No significant effect
Temperature and initial degradation and mineralisation	15–78 °C, 5.5 ppm C solutions	Fluctuating results. Approximately 2 fold difference between minimum and maximum rates
Light intensity and initial degradation and mineralisation	15.5 ppm C solutions	Transition point: 1.22×10^{-5} einsteins s^{-1} Low light intensities: directly proportional to light intensity High light intensities: the rate of initial degradation increases in proportion to light intensity to a power of 0.12 and the rate of mineralisation rises in proportion to light intensity to the power of 0.58 Quantum yields: 0.003–0.039 mol of carbon per photon
Oxygen and adsorption	Under oxygen, nitrogen and aerated conditions, 15 ppm C solutions	Little effect
Oxygen and initial degradation	0–100% oxygen, 20 ppm C solutions	Did not follow standard Langmuir–Hinshelwood kinetics. Degradation even under nitrogen
Oxygen and mineralisation	0–100% oxygen, 20 ppm C solutions	Mineralisation even under nitrogen
pH and mineralisation	15 ppm solutions, pH 2–11.8	The maximum mineralisation rate was observed at pH 7. In the acidic region the rate was lowest at pH 4 and in the alkali region the lowest rate was observed at pH 9

which could be mineralised in the presence of alternative metal ion electron acceptors [13].

3.6. pH

3.6.1. Adsorption

This was not performed due to the high insolubility of humic acid above pH 6.

3.6.2. Mineralisation rates

Due to insolubility problems only mineralisation rates were determined; the carbon dioxide was purged off after acidification (Fig. 6). The maximum mineralisation rate was observed at pH 7 (close to pH_{zpc}) [29,30]. The rate was slower after adding either acid or alkali. In the acidic region the rate was lowest at pH 4 and in the alkali region the lowest rate was observed at pH 9, which is close to the two pK_a values for titanium dioxide.

In alkali conditions the carboxyl groups on the humic acid will be ionised. A majority of phenolic groups will only be ionised above pH 9. This ionisation will lead to a negative charge on the humic acid molecules, which would lead to a repulsion from the increasingly more negative titanium dioxide (above the pH_{zpc}) The lowered adsorption should lead to a reduced rate as observed. The slight increase at higher pH values may be due to the enhancement of indirect oxidation pathways via the oxidation of hydroxide ions. With decreasing pH the phenolic and carboxyl groups will become increasingly un-ionised; this may allow greater adsorption on titanium dioxide as electrostatic repulsion will be reduced, but aggregation may be a major problem leading to lower mass transport rates and a lower surface area for light adsorption (this was observed in the acidic solutions where the titanium dioxide and humic acid suspensions precipitated rapidly when stirring ceased). The effect of pH on the band edges of the semiconductor and the oxidation potential of humic acid is hard to predict.

A very similar profile was observed by Coleman et al. [31] in the semiconductor degradation of 17β-oestradiol. Bekbolet et al. [5] obtained their highest rates of initial degradation (in terms of colour and DOC) in acid conditions. No mention of solubility problems were made.

3.7. Conclusion and further work

Our aim was to investigate the effect of the several operational parameters on the adsorption, the initial degradation and steady state mineralisation of Aldrich humic acid during semiconductor photocatalysis. A summary of the most pertinent results are given in Table 3.

We set out to apply the standard equations based upon Langmuir–Hinshelwood kinetics that are often used in the analysis of semiconductor experiments. We discovered that the data did not often fit the models well and decided that this was due to the heterogeneity of humic acid and its large molecular size. The high adsorption of humic acid onto titanium was thought to influence the rates of degradation more significantly than for other compounds. In the future we may have to resort to using factorial equations or neural networks to model the complex kinetics demonstrated by such compounds.

Acknowledgements

I would like to acknowledge all the staff of the University of Ulster, Prof. Mills for his role as my D.Phil. external, and DENI for providing financial assistance.

References

[1] H.-R. Schulten, B. Plage, M. Schnitzer, Naturwissenschaften 78 (1991) 311.
[2] B.R. Eggins, F.L. Palmer, J.A. Byrne, Water Res. 31 (1997) 1223.
[3] S. Ogawa, M. Tanigawa, M. Fujioka, Y. Hanasaki, Jpn. J. Toxicol. Environ. Health 41 (1995) 7.
[4] M. Bekbolet, G. Ozkoswman, Water Sci. Technol. 33 (1996) 189.
[5] M. Bekbolet, M. Cecen, G. Ozkosemen, Water Sci. Technol. 34 (1996) 65.
[6] M. Bekbolet, J. Environ. Sci. Health Part A 31 (1996) 845.
[7] M. Bekbolet, I. Balcioglu, Water Sci. Technol. 34 (1996) 73.
[8] P. Backlund, L. Kronberg, L. Tikkanen, Chemosphere 17 (1988) 1329.
[9] A. Parker, Proc. Roy. Soc. London A 220 (1953) 104.
[10] G. Hatchard, C.A. Parker, Proc. Roy. Soc. London A 235 (1956) 518.
[11] H.Y. Chen, O. Zahraa, M. Bouchy, F. Thomas, J.Y. Botero, Photochem. Photobiol. A 85 (1995) 179.
[12] J. Cunningham, G. Al-Sayyed, S. Srijaranai, in: G.R. Helz, R.G. Zepp, D.G. Crosby (Eds.), Aquatic and Surface Photochemistry, Lewis Publishers, USA, 1994, pp. 317–346.
[13] Results yet to be published.
[14] J.A. Bryne, D.Phil. Thesis, University of Ulster, 1997.
[15] R.W. Matthews, J. Mc Evoy, Photochem. Photobiol. A 64 (1992) 231.
[16] N. Serpone, R. Terzian, C. Minero, E. Pelizzetti, in: Photosensitive Metal-Organic Systems, American Chemical Society, Washington, DC, 1993, pp. 281–341.
[17] R. Terzian, N. Serpone, J. Photochem. Photobiol. A 89 (1995) 163.
[18] A. Mills, C.E. Holland, R.H. Davies, D. Worsley, J. Photochem. Photobiol. A 83 (1994) 257.
[19] A. Mills, S. Morris, R.J. Davies, Photochem. Photobiol. A 70 (1993) 183.
[20] J. Moser, M. Gratzel, J. Am. Chem. Soc. 105 (1983) 6547.
[21] A. Mills, R.J. Davies, Photochem. Photobiol. A 85 (1995) 173.
[22] H. Al-Ekabi, N. Serpone, in: N. Serpone, E. Pelizzetti (Eds.), Photocatalysis, Fundamentals and Applications, Wiley, Chichester, 1989, p. 457.
[23] K. Okamoto, Y. Yamamoto, H. Tanaka, A. Itaya, Bull. Chem. Soc. Jpn. 58 (1985) 2023.
[24] V. Augugliaro, V. Loddo, G. Marci, L. Palmisano, M.J. Lopez-Munoz, J. Catal. 166 (1997) 272.
[25] A. Mills, R.H. Davies, D. Worsley, Chem. Soc. Rev. (1993) 417.
[26] C. Kormann, D.W. Bahnemann, M.R. Hoffmann, Environ. Sci. Technol. 25 (1991) 494.
[27] S. Upadhya, D.F. Ollis, J. Phys. Chem. 101 (1997) 2625.
[28] B. Brendan, Final Year Project, Dept. ABCS, University of Ulster at Jordanstown, 1995.
[29] Y. Ku, R.-M. Leu, K.-C. Lee, Water Res. 30 (1996) 2569.
[30] J. Zhao, A. Hidaka, E. Takamura, E. Pelizzetti, N. Serpone, Langmuir 9 (1993) 1646.
[31] H.M. Coleman, B.R. Eggins, J.A. Byrne, F.L. Palmer, Appl. Catal. B 24 (2000) 1.